DOE/ET-53088-379-R IFSR #**379-R**

Statistical-Mechanical Theory of Cold Nuclear Fusion in Metal Hydrides

Setsuo Ichimaru,[1] *Aiichiro Nakano,*[1] *Shuji Ogata,*[1] *Shigenori Tanaka,*[1]
Hiroshi Iyetomi,[1] and *Toshiki Tajima*
Department of Physics and Institute for Fusion Studies
The University of Texas at Austin
Austin, Texas 78712

September 1989

[1] *Dept. of Physics, University of Tokyo, Bunkyo-ku, Tokyo 113, Japan*

Statistical-Mechanical Theory of Cold Nuclear Fusion in Metal Hydrides

Setsuo ICHIMARU, Aiichiro NAKANO, Shuji OGATA,
Shigenori TANAKA, Hiroshi IYETOMI and Toshiki TAJIMA†

Department of Physics, University of Tokyo, Bunkyo-ku, Tokyo 113
†*Department of Physics and Institute for Fusion Studies,*
University of Texas, Austin , TX78712, U.S.A.

(Received July 17, 1989)

Screening action of the s-d hybridized electrons in PdH_x and TiH_x is analyzed in the Fermi-Thomas approximation. The resulting interaction between hydrogen exhibits an attractive part arising from interference between the H-induced s-electrons and the valence electrons. The screening potentials due to many-body effects between the electron-screened protons are examined through solution to the hypernetted-chain equations. The nuclear reaction rates between hydrogen isotopes are calculated at various temperatures by taking account of statistical-mechanical enhancement arising from the increment in the Coulombic chemical potential of a reacting pair before and after nuclear reaction. Remarkable isotopic and temperature-dependent effects are predicted.

PACS numbers: 71.45.-d, 24.90.+d

§1. Introduction

Possibility of nuclear fusion reactions between hydrogen isotopes in metal hydrides (MH_x) through electrolysis[1,2] or through absorption/desorption processes[3] has created a challenge to condensed matter physics, calling for a theoretical account of how two hydrogen nuclei can come to fuse by overcoming the Coulombic repulsive forces in such a metallic environment. Experiments[4,5] performed under analogous settings, on the other hand, have not shown significant observation of nuclear reactions. One therefore anticipates the rates of nuclear reactions depending quite delicately on the states of reacting pairs at short distances.

The quantities that essentially control the penetration probability and its enhancement for nuclear reactions between hydrogen isotopes are the screening potentials,[6,7]

$$H(r) = v(r) + \ln[g(r)]/\beta, \tag{1}$$

which result from many-body effects in statistical mechanics. Here, β is the inverse temperature in energy units, $v(r)$ is the potential of binary interaction, and $g(r)$ is the associated two-particle (radial) distribution function. The last term of eq. (1) is minus the potential of mean force;[8] the screening potential (1) is represented diagrammatically in Fig. 1. It has been shown[6,9] that the value of $H(r)$ at $r = 0$ is equal to the increment in the interaction (or excess) part of the chemical potential for the reacting pair before and after the nuclear reaction. It then follows[6,7,9] that the reaction rate is enhanced by a factor, $\exp[\beta H(0)]$. (See also §4 below.)

In this paper we present a set of careful analyses on the screening potentials in Pd and Ti, two of the typical metals used in "cold fusion" experiments. We

thus carry out Fermi-Thomas analyses on screening action of the s-d hybridized electrons coupled with the f-sum rules, calculate effective masses of such screening electrons, and thereby derive charge-form factors on ionic nuclei in PdH_x and TiH_x. The resulting hydrogen interaction, containing an attractive part due to strongly coupled valence electrons, depends sensitively on x and E_S, the energy levels of those s-electron states which are induced by hydrogen around the octahedral sites (Pd) or the tetrahedral sites (Ti) of the fcc crystals. The effective interactions between hydrogen in those metals differ substantially, in that Pd has a large number (ten per atom) of outer-shell d-electrons, while Ti can have a large value (two if all the tetrahedral sites are occupied) of x, the relative atomic concentration of hydrogen to metal. The screening actions of the electrons significantly influence the nulear reaction rates at room temperatures.

Many-body effects between the screened protons are then taken into account through a solution to the hypernetted-chain (HNC) equations,[7,8] for the repulsive part and through examination of possible quasi-bound states and elastic scatterings for the attractive part of the binary interaction. Resulting rates of nuclear reactions are calculated for combinations of hydrogen isotopes at various temperatures. Remarkable density- and temperature-dependent effects as well as isotopic effects are predicted.

§2. Screening Effects of Electrons

We begin with an f-sum rule expression for the frequency-dependent dielectric function,[10]

$$\epsilon(\omega) = 1 - \sum_j \frac{4\pi n_j e^2}{m} \frac{1}{\omega^2 - \omega_j^2}, \tag{2}$$

where m is the bare mass of an electron, n_j and $E_j = \hbar\omega_j$ refer to the number density and excitation energy of the electrons in the j-level.

Since $\omega \ll \omega_j$ at room temperatures, the dielectric constant of our concern is

$$\epsilon(0) = 1 + 4\pi e^2 \hbar^2 \sum_j n_j / m E_j^2. \tag{3}$$

This formula indicates that the contribution of $(4s)^2(4p)^6$ electrons in the Kr-core of Pd with binding energies, 86.4 eV and 51.1 eV (ref. 11), respectively, produces a core-dielectric constant $\epsilon_c = 1.25$ for the number density of palladium, $n_{Pd} = 6.25 \times 10^{22} cm^{-3}$, corresponding to a lattice constant, 4 Å. For Ti, $\epsilon_c = 1.36$, from $(3s)^2(3p)^6$ electrons in the Ar-core at 60.3 eV and 34.6 eV (ref. 11) if $n_{Ti} = 4.7 \times 10^{22} cm^{-3}$ is assumed.

Photoemission studies[12,13] of the Pd/H system have shown a band of hydrogen-induced energy states centered at about 1 eV below the bottom of Pd-derived 4d bands of width 4.4 eV. Analogous studies[14] of the Ti/H system have shown a broad band of H-induced s-states centered at about 3.3 eV below the bottom of Ti-derived 3d bands of width 1.7 eV. The energy levels E_S of the s-state electrons below the Fermi surface quantify trapping characteristics of where the hydrogen sits (octahedral sites in Pd and tetrahedral sites in Ti).

We analyze the screening effect of s-d hybridized electrons by separating the electrons in metallic d-band into ζ_d (per atom) *screening* electrons and the remaining *valence* electrons. The latter electrons are those occupying the states near the Fermi surface; observations[12-14] of the density of states and the specific heats have indicated their effective masses in the vicinity of the bare mass. Analogously we separate H-induced s-electrons into ζ_S (per atom) screening electrons and $1 - \zeta_S$ valence electrons. The total number density of

the s-d hybridized screening electrons is therefore $(\zeta_d + x\zeta_S)n_M$, where n_M is the number density of metal atoms; $\zeta_d \simeq 8$ for Pd, and $\zeta_d \simeq 1$ for Ti.

The values of E_S play a central part in the analysis on the screening of H-induced s-electrons hybridized with metal-derived d-electrons. We derive a wave number-dependent charge-form factor of the protons with the screening electrons in the Fermi-Thomas approximation[15] as

$$\phi(k) = 1 - \zeta_S + \zeta_S k^2/(k^2 + \kappa^2). \tag{4}$$

The value of ζ_S can be determined through a consideration of a partial system of hydrogen and its ζ_S screening and $(1 - \zeta_S)$ valence electrons. Since $1 - \zeta_S$ corresponds to an effective strength of electric charge that remains statically to hydrogen after being screened by ζ_S electrons, it must be equal to the inverse of the dielectric constant (3) arising from the ζ_S electrons, i.e.,

$$(1 - \zeta_S)^{-1} = 1 + 4\pi x \zeta_S n_M e^2 \hbar^2/mE_S^2. \tag{5}$$

The remaining charge $1 - \zeta_S$ will be screened naturally by the valence electrons.

In the Fermi-Thomas approximation, the screening constant of the s-d hybridized electrons with an effective mass m_S is calculated as[15]

$$\kappa = [12\pi e^2 m_S/(3\pi^2)^{2/3}\hbar^2]^{1/2}[(\zeta_d + x\zeta_S)n_M]^{1/6}.$$

The screening constant of ζ_S Bohr electrons, on the other hand, is given by $\zeta_S m_S e^2/\hbar^2$. Equating these two, we find

$$\kappa = 12[(\zeta_d + x\zeta_S)n_M]^{1/3}/(9\pi)^{1/3}\zeta_S. \tag{6}$$

In Tables I and II, the values of ζ_S and κ^{-1} are listed for relevant combinations of x and E_S in PdH_x and TiH_x.

The potential of binary interaction between the screened protons is thus expressed in Fourier components as

$$\tilde{\Phi}(k) = 4\pi[e\phi(k)]^2/k^2\epsilon_c\epsilon_v(k), \tag{7}$$

where $\epsilon_v(k)$ represents the dieletric screening function[7,16] of the valence electrons; in the ensuing calculations we assume the effective valence Z_e per a metal atom to be three. The r_S parameter of the valence electrons is given by

$$r_S = (3/4\pi Z_e n_M)^{1/3} m_v e^4/\hbar^2 \tag{8}$$

with m_v representing the effective mass of valence electrons. Assuming $m_v \simeq m$, we find $r_S = 2 \sim 3$. Screening effects of those valence electrons will thus create attractive interactions between hydrogen at short distances when the local-field effects[7] produced by strong electron-electron correlations are appropriately taken into account. In the absence of screening, i.e., in the limits $\phi(k) \to 1$ and $\epsilon_v(k) \to 1$, eq. (7) reduces naturally to the bare Coulombic contribution, $4\pi e^2/\epsilon_c k^2$, in the dielectric medium with ϵ_c.

Figure 2 shows examples of $\Phi(r)$, the inverse Fourier transform of $\tilde{\Phi}(k)$, in Pd and Ti. An attractive part is created at outside the screening s-electrons as a consequence of interference with the valence electrons in eq. (7), The electronic contribution U_e to the screening potential in $\Phi(r)$ is evaluated as

$$U_e = \lim_{r \to 0}[e^2/\epsilon_c r - \Phi(r)]. \tag{9}$$

The values of U_e, listed in Tables I and II, take on magnitude sufficiently large as to influence the nuclear reation rates at room temperatures. Listed also in those tables are: r_1, the radius at which $\Phi(r)$ first vanishes; r_m, the radius at

the first minimum, where $\Phi(r_m) = -\Phi_m$; $\Phi''_m = d^2\Phi(r_m)/dr_m^2$; r_2, the radius at which $\Phi(r)$ next vanishes; r_h, the radius at the first maximum (hump), where $\Phi(r_h) = \Phi_h$. Both r_1 and r_m are greater for Ti than for Pd, leaving sizable many-body effects in Ti.

At room temperatures, the Gamow penetration factors between hydrogen isotopes, a and b (= p, d, t), taking account of the electronic screening, are calculated approximately as

$$P_{ab} = \exp\{-(2/\hbar)\int_0^{r_1} dr[2M_{ab}\Phi(r)]^{1/2}\}. \tag{10}$$

An isotopic effect enters eq. (10) through the reduced mass, M_{ab}. Nuclear rection rates per a pair of a and b are then obtained as

$$\lambda_{ab}^{(0)} \simeq 10^{10} S_{ab}(\mathrm{keVb}) P_{ab}/[M_{ab}(\mathrm{amu})T(\mathrm{K})]^{1/2} \ \ (\mathrm{s}^{-1}). \tag{11}$$

Here, we assume the larger of n_a and n_b to be $6\times10^{22}cm^{-3}$, $S_{dd} = 106$ (ref. 17), $S_{dt} = 1.7\times10^4$ (ref. 18), $S_{pd} = 2.5\times10^{-4}$ (ref. 19), and $S_{pp} = 4\times10^{-22}$ (ref. 19). The weak dependence of eq. (11) on T comes from statistics of relative velocities between reacting particles; in the ensuing calculations of eq. (11) we assume $T = 300$K. The values of $\lambda_{dd}^{(0)}$, plotted in Figs. 3 and 4, are larger for Pd than for Ti due to the differences in U_e and r_1. The latter stem mainly from the differences in ζ_d.

§3. Many-Body Effects in Hydrogen

The nuclear reaction rates (11) have not taken into account the statistical-mechanical effects arising from multiple interaction generated by $\Phi(r)$. To calculate $\beta H(0)$ in the diagrammatic summation of Fig. 1 where $v(r) = \Phi(r)$, we

split the latter into the repulsive and attractive parts, $\Phi(r) = \Phi_R(r) + \Phi_A(r)$, so that

$$\Phi_R(r) = (e^2/\epsilon_c r)\Big[\exp(-r/D_S) + (r/\rho_R)^p \exp(-r/D_R)\Big], \tag{12}$$

$$\Phi_A(r) = -(e^2/\epsilon_c r)(r/\rho_A)^q \exp(-r/D_A). \tag{13}$$

The parameters in eqs. (12) and (13), listed in Tables III and IV, are determined so that the values of U_e, r_1, Φ_m and the first hump of $\Phi(r)$ at $r \simeq 2$Å are accurately reproduced.[20] In Fig. 5, we show examples of comparison between the original and fitted values for $\Phi(r)$.

Corresponding to the splitting of the binary potential into the repulsive and attractive parts, we factor the two-particle distribution function in eq. (1) as

$$g(r) = g_R(r) g_A(r), \tag{14}$$

so that

$$g_{R(A)}(r) = \exp\{-\beta[\Phi_{R(A)}(r) - H_{R(A)}(r)]\}. \tag{15}$$

In eqs. (14) and (15), the screening potential has been split analogously into two parts: $H(r) = H_R(r) + H_A(r)$. The repulsive contribution $H_R(r)$ is calculated by summing the diagrams as in Fig. 1 where *all* the bonds are $f_R(r) = \exp[-\beta\Phi_R(r)] - 1$; $H_A(r)$ then collects all the remaining diagrams, in which at least one of the bonds are $f_A(r) = \exp[-\beta\Phi_A(r)] - 1$.

Quantum-mechanical treatment is particularly essential for the calculation of $H_A(r)$; an attractive potential of magnitude, eq. (13), if treated classically, would create anomalously sharp and unphysical peaks in $g(r)$. We thus take up an enhancement factor $\exp[\beta H_A(0)]$ arising from the attractive part by a

consideration of possible formation of quasi-bound pairs at the potential troughs characterized by the parameters, r_m, Φ_m, and Φ_m'' (Tables I and II). Near the bottom of the potential trough, a hydrogen atom may assume a state of harmonic oscillators with energies, $\hbar(\nu+1/2)(\Phi_m''/M_{ab})^{1/2}$, where $\nu = 0, 1, 2 \ldots$. For the state of zero-point oscillation ($\nu = 0$), we approximately calculate

$$\exp[\beta H_A(0)] \simeq 1+\exp\{-(M_{ab}\Phi_m'')^{1/2} r_m^2/\hbar+\beta[\Phi_m-(\hbar/2)(\Phi_m''/M_{ab})^{1/2}]\}. \quad (16)$$

For all the combinations (25 cases) of x and E_S considered in PdH_x and TiH_x, we found $\exp[\beta H_A(0)] \simeq 1$ at $T = 300$K; little enhancement comes from quasi-bound pairs due to the magnitude of r_m.

We next consider the effects of non-resonant elastic scatterings by the attractive potential well $\Phi_A(r)$. In the limit of low energies,[22] the effective scattering length is given approximately by $2D_A$. When the temperatutre is finite, the latter is superseded by $\Lambda_{ab} = (2\pi\hbar^2\beta/M_{ab})^{1/2}$, the thermal de Broglie wavelength, if $\Lambda_{ab} < 2D_A$. Upper bounds of the effective "packing fractions", $\eta_{max} = \Lambda_{ab}^3 x n_M$, then do not exceed 0.1 in all the cases examined here. In light of the equations of states for equivalent hard-sphere systems,[8,9] we derive

$$\beta H(0)_{HS} = \eta(8 - 9\eta + 3\eta^2)/(1 - \eta)^3, \quad (17)$$

so that we conclude that enhancement of reaction rates due to elastic scattering by the attractive part of the binary potential is negligible.

Finally we investigate the statistical-mechanical enhancement factor $\exp[\beta H_R(0)]$ arising from elastic scatterings by the repulsive part $\Phi_R(r)$ of the binary interaction. For this, we first note that the thermal contact distances d_0, determined from $2\beta\Phi_R(d_0) = 1$, take on values significantly larger than the

shortest distances between tetrahedral sites ($\sim$ 2.2Å) for Ti, where hydrogen sits; typically, $d_0 = 2.8$Å (in TiH_x) for E_S=5 eV at $T = 300$K. Ample strength of the potential therefore remains at those inter-site distances to justify consideration of many-body effects for hydrogen in TiH_x. On the other hand, $d_0 = 2.5$Å in PdH for $E_S = 5$ eV at $T = 300$K; this is shorter than the distance between octahedral sites ($\sim$ 2.8Å) for Pd. There may not remain much strength in the potential for many-body interaction between hydrogen in PdH_x.

We approach the increment in the interaction chemical potential through a solution[23] to the HNC equations, known to be accurate in describing statistical properties of long-ranged Coulmbic systems. In so doing, we examine a possible quantum-mechanical correction to $\Phi_R(r)$ in eq. (12), arising from S-wave scattering between a and b. Since the last term in eq. (12) determines d_0 in the cases of our concern, a factor of $[1+1.225(\Lambda_{ab}/d_0)^2]/[1+(\Lambda_{ab}/d_0)^2]$ should be multiplied to the D_R for the quantum correction. This correction, however, turns out to be negligible in magnitude for all the cases treated here.

The HNC values, $\beta H_R(0)_{HNC}$, of the screening potential overestimate the true values by its neglect of the bridge-diagram contributions[8]; the latter exert repulsive forces at short distances. For Coulombic systems, the true values may be obtained[24] by $\beta H_R(0) = 0.866[\beta H_R(0)_{HNC}+1]$ in a strong-coupling regime where $\beta H_R(0) > 8$. In this regime, the resulting values of $\beta H_R(0)$ can then be parametrized accurately in a form,

$$\beta H_R(0) = \frac{1.057\beta e^2}{\epsilon_c a}\left[\exp\left(\frac{-a}{D_S}\right) + \left(\frac{1.09a}{\rho_R}\right)^p \exp\left(\frac{-1.06a}{D_R}\right)\right], \qquad (18)$$

where $a = (3/4\pi x n_M)^{1/3}$. In the bare-Coulomb limit ($D_S \to \infty$ and $\rho_R \to \infty$), eq. (18) reproduces the ion-sphere contribution to the chemical-potential increment derived originally by Salpeter and Van Horn[6] for dense steller matter.

When D_S is finite, the exponential screening factor in the first term of eq. (18) suppresses the hydrogen interaction and thereby enhancement of nuclear reactions. The newly created second term additionally accounts for the many-body effects in the nuclear reactions.

§4. Rates of Cold Nuclear Fusion

The rate of nuclear reaction is proportional to overlapping of wave functions for the two reacting particles at zero separation, which is $g(0)$ evaluated quantum-mechanically. Equation (14), based on classical considerations as in Fig. 1, needs therefore to be modified appropriately.

To do so, we rewrite eq. (14) or Fig. 1 as

$$g(r) = \exp[-\beta\Phi(r)]\exp[\beta H(r)]. \tag{19}$$

It is clear that the quantum-mechanical counterpart to the first factor on the right-hand side of eq. (19) at $r = 0$ is given by the penetration probability (10). Since the contributions from the second factor have been treated quantum-mechanically in the preceding section, we may thus calculate the nuclear reaction rates according to

$$\lambda_{ab} = \lambda_{ab}^{(0)}\exp[\beta H(0)]. \tag{20}$$

where $H(0)$ is evaluated as a summation between eqs. (16) and (18). Computed results for the reaction rates in PdH_x and TiH_x at temperatures, T(K)=200, 300, and 600, are shown in Figs. 3 and 4 for various combinations of x and E_S. Enhancement by the many-body effect decreases steeply with T as eq. (18) illustrates.

Figures 3 and 4 appear to imply that the reaction rates suggested by experiments[2,3] cannot be accounted for by the calculations described above. In addition we remark that the periodic lattice potentials, which are ignored in the present theory, may act to equilibrate the hydrogen atoms in the vicinity of their individual sites at low temperatures, and may thus hinder their approach to a mutual distance near r_1, necessary for nuclear reactions to take place.

The steep variation of eq. (18) on a implies, on the other hand, that if a mechanism unaccounted for in the foregoing treatments is operative in the metal hydrides so that an *effective* short-range separation between a pair of hydrogen atoms assumes a value smaller than a, then the reaction rates would be enhanced over the values cited in Figs. 3 and 4. If, for example, we assume $a = 0.5$Å in eq. (18), the resulting λ_{dd} in eq. (20) for PdH with $E_S = 5$ eV would take on $\sim 10^{-21}$ (s^{-1}); similarly with an assumption of $a = 0.6$Å, we find $\lambda_{dd} \simeq 10^{-20}$ (s^{-1}) for TiH_2 with $E_S = 5$ eV. Those are close to the values suggested in the experiments.[2,3]

A number of physical mechanisms exist in creating such a local variation of hydrogen concentration in actual metal hydrides. The periodic potential structure of metallic atoms has a strength sufficient to produce a local density modulation of such a magnitude. Lattice defects, which usually exist, may further enhance the probability of two hydrogen atoms approaching close to one another. In transient non-equilibrium situations,[2,3] some of the equilibration constraints may be relaxed so that increased number of hydrogen atoms collide with each other frequently near the low-E_S sites and/or in the lattice defects. For a quantitative estimate on these effects, we must proceed with microscopic analyses on how lattice fields (and their defects) actually influence the many-body effects between hydrogen.[25]

A remarkable prediction in the present theory is isotopic effect in nuclear reactions (Fig. 6). Since the Coulombic chemical potential (and its increment, eq. (18)) is independent of the reduced mass, the isotopic effects enter the reaction rates through S_{ab} and P_{ab} in eq. (11). Although the binary potential $\Phi(r)$ has been lowered considerably by the electronic screening, the quantity in the exponent of eq. (10) still takes on a large negative value, resulting in remarkable isotopic effects which should favor reactions involving light species (i.e., protons). In Fig. 6, the rates of p-d reactions substantially exceed those of d-d, and the rare weak interaction of p-p may even catch up with d-t. Those isotopic effects, if detectable experimentally, should be more pronounced in Ti than in Pd, since TiH_x can have a larger x and a larger spatial extent of hydrogen interaction.

Acknowledgments

The work was supported in part through Grants-in-Aid for Scientific Research by the Ministry of Education, Science and Culture, and by the U. S. Department of Energy.

References

1) M. Fleischmann, S. Pons, and M. Hawkins: J. Electroanalytical Chem. **261** (1989) 301.

2) E. S. Jones, E. P. Palmer, J. B. Czirr, D. L. Decker, G. L. Jensen, J. M. Thorne, S. F. Taylor, and J. Rafelski: Nature **338** (1989) 737.

3) A. De Ninno, A. Frattolillo, G. Lollobattista, L. Martins, L. Mori, S. Podda, and F. Scaramuzzi: submitted to Europhys. Lett.

4) J. F. Ziegler, T. H. Zabel, J. J. Cuomo, V. A. Brusic, G. S. Cargill, III, E. J. O'Sullivan, and A. D. Marwick: Phys. Rev. Lett. **62** (1989) 2929.

5) M. Gai, S. L. Rugari, R. H. France, B. J. Lund, Z. Zhan, A. J. Davenport, H. S. Isaacs, and K. G. Lynn: submitted to Nature.

6) E. E. Salpeter: Aust. J. Phys. **7** (1954) 373; E. E. Salpeter and H. M. Van Horn: Astrophys. J. **155** (1969) 183; H. E. DeWitt, H. C. Graboske, and M. S. Cooper: Astrophys. J. **181** (1973) 439.

7) For a review, see S. Ichimaru: Rev. Mod. Phys. **54** (1982) 1017.

8) For a general reference, see J. P. Hansen and I. R. MacDonald: *Theory of Simple Liquids, 2nd Ed.* (Academic, London, 1986).

9) W. G. Hoover and J. C. Poirer: J. Chem. Phys. **37** (1962) 1041; B. Widom: J. Chem. Phys. **39** (1963) 2803; B. Jancovici: J. Stat. Phys. **17** (1977) 357; Y. Rosenfeld and N. W. Aschcroft: Phys. Rev. A**20** (1979) 1208.

10) D. Pines: *Elementary Excitations in Solids* (Benjamin, N. Y., 1963), Sec. 4-2.

11) J. A. Beardeen and A. F. Burr: Rev. Mod. Phys. **39** (1967) 125.

12) D. E. Eastman, J. K. Cashion, and A. C. Switendick: Phys. Rev. Lett. **27** (1971) 35.

13) See also F. E. Wagner and G. Wortmann: in *Hydrogen in Metals I: Basic Properties*, edited by G. Alefeld and J. Völkl (Springer, Berlin, 1978), p. 131.

14) S. A. Nemnonov and K. M. Kolobova: Fiz. Metal Metalloved **22** (1966) 680; D. E. Eastman, Solid State Commum. **10** (1972) 933; A. C. Switendick, J. Less-Common Metals **49** (1976) 283.

15) Reference 10, Sec. 3-3.

16) J. Hafner: *From Hamiltonian to Phase Diagrams* (Springer, Berlin, 1987), pp. 34-66; for a specific formula for $\epsilon_v(k)$, see S. Ichimaru and K. Utsumi: Phys. Rev. B**24** (1981) 7385.

17) M. Jarmie and R. E. Brown: Nuc. Inst. Meth. B**10/11** (1985) 405; J. Rafelski, M. Gajta, D. Harley, and S. E. Jones: to be published.

18) J. D. Jackson: Phys. Rev. **106** (1957) 330.

19) J. N. Bahcall and R. K. Ulrich: Rev. Mod. Phys. **60** (1988) 297.

20) This fitting with two exponential functions in eq. (12) is more accurate than that in a preliminary report[21)], where the repulsive part was represented by a single screened-Coulombic term.

21) S. Ichimaru, A. Nakano, S. Ogata, S. Tanaka, H. Iyetomi, and T. Tajima: unpublished.

22) For example, L. D. Landau and E. M. Lifshitz: *Quantum Mechanics: Non-Relativistic Theory, 2nd Ed.* (Pergamon, Oxford, 1965), Sec. 130.

23) K. C. Ng: J. Chem. Phys. **61** (1974) 2680; S. Tanaka and S. Ichimaru: J. Phys. Soc. Jpn **53** (1984) 2039.

24) H. Iyetomi and S. Ichimaru: Phys. Rev. A**27** (1983) 3241.

25) S. Ichimaru, S. Ogata, A. Nakano, H. Iyetomi, and T. Tajima: to be published.

Figure Captions

Fig. 1. Diagrammatic representation of the screening potential. Dashed lines are the f-bonds, $f(r) = \exp[-\beta v(r)] - 1$, and solid circles are the particle coordinates to be integrated.

Fig. 2. Binary interaction potentials between electron-screened protons in metal hydrides at $E_S = 5$ eV.

Fig. 3. The d-d reaction rates in PdH_x. $\lambda_{dd}^{(0)}$ refer to the rates without the statistical-mechanical enhancement; E_S are in units of eV; connecting lines are to guide the eye.

Fig. 4. The d-d reaction rates in TiH_x. Otherwise, the same as in Fig. 3.

Fig. 5. Interaction potentials, $\Phi(r)$, in PdH and TiH_2 at $E_S = 4$ eV. The solid curves are calculated from eq. (7); the dashed curves, from eqs. (12) and (13).

Fig. 6. Isotopic effects of nuclear reaction rates in PdH (open circles) and TiH_2 (solid circles) at $E_S = 5$ eV.

Table I. Screening and interaction parameters in PdH_x.

E_S (eV)	x	ζ_S	κ^{-1} (Å)	U_e (eV)	r_1 (Å)	r_m (Å)	Φ_m (eV)	Φ''_m (eVÅ^{-2})	r_2 (Å)	r_h (Å)	Φ_h (eV)
4	3/4	0.75	0.25	58.2	0.59	0.81	0.38	7.9	1.64	1.90	0.017
	1	0.81	0.27	56.8	0.57	0.79	0.48	9.9	1.66	1.91	0.017
5	3/4	0.61	0.21	61.8	0.72	0.94	0.16	3.5	1.57	1.87	0.020
	1	0.71	0.24	59.2	0.62	0.84	0.31	6.4	1.63	1.90	0.017

Table II. Screening and interaction parameters in TiH_x.

E_S (eV)	x	ζ_S	κ^{-1} (Å)	U_e (eV)	r_1 (Å)	r_m (Å)	Φ_m (eV)	Φ''_m (eVÅ^{-2})	r_2 (Å)	r_h (Å)	Φ_h (eV)
4	1	0.75	0.42	34.2	0.73	1.00	0.46	6.7	1.95	2.20	0.015
	3/2	0.84	0.43	35.2	0.70	0.97	0.52	7.5	1.95	2.20	0.016
	2	0.88	0.43	36.4	0.68	0.94	0.55	7.9	1.92	2.19	0.017
5	1	0.61	0.34	36.3	0.77	1.03	0.33	5.1	1.86	2.14	0.020
	3/2	0.74	0.39	36.5	0.71	0.98	0.44	6.6	1.90	2.17	0.017
	2	0.81	0.39	37.4	0.69	0.95	0.49	7.3	1.90	2.17	0.018

Table III. Fitting parameters in eqs. (12) and (13) for PdH_x.

E_S (eV)	x	D_S (Å)	p	ρ_R (Å)	D_R (Å)	q	ρ_A (Å)	D_A (Å)
4	3/4	0.20	8.3	1.04	0.19	2.5	0.71	0.23
	1	0.20	7.6	1.05	0.20	2.5	0.66	0.23
5	3/4	0.19	10.9	1.07	0.16	4.8	0.64	0.16
	1	0.19	8.9	1.04	0.18	2.7	0.74	0.23

Table IV. Fitting parameters in eqs. (12) and (13) for TiH_x.

E_S (eV)	x	D_S (Å)	p	ρ_R (Å)	D_R (Å)	q	ρ_A (Å)	D_A (Å)
4	1	0.31	11.4	0.96	0.16	3.1	0.59	0.24
	3/2	0.30	10.4	0.98	0.17	3.0	0.59	0.25
	2	0.29	9.7	1.00	0.18	2.9	0.59	0.25
5	1	0.29	11.6	1.02	0.16	3.5	0.60	0.22
	3/2	0.29	10.4	1.01	0.17	3.1	0.60	0.24
	2	0.28	10.0	1.00	0.17	2.9	0.61	0.25

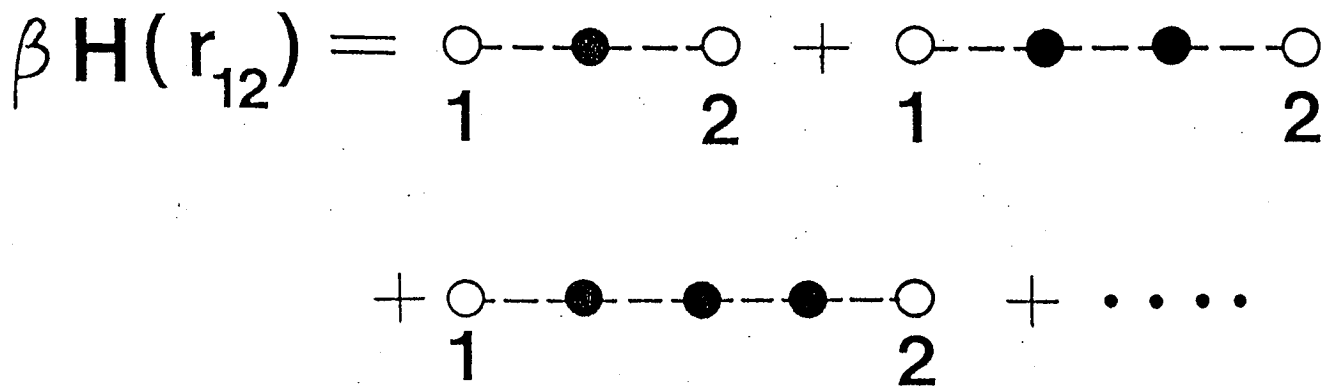

Fig. 1 S. Ichimaru et al.

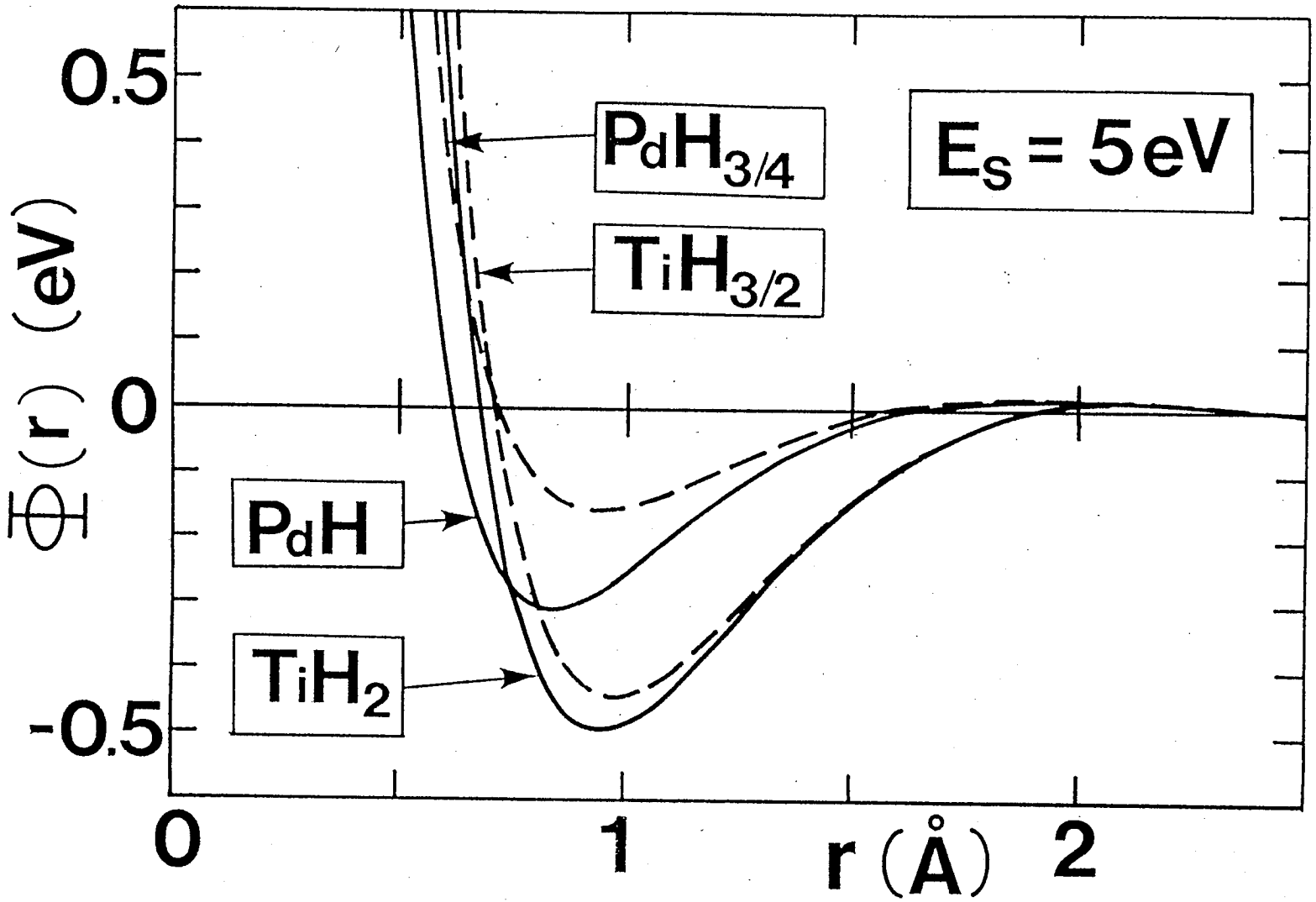

Fig. 2 S. Ichimaru et al.

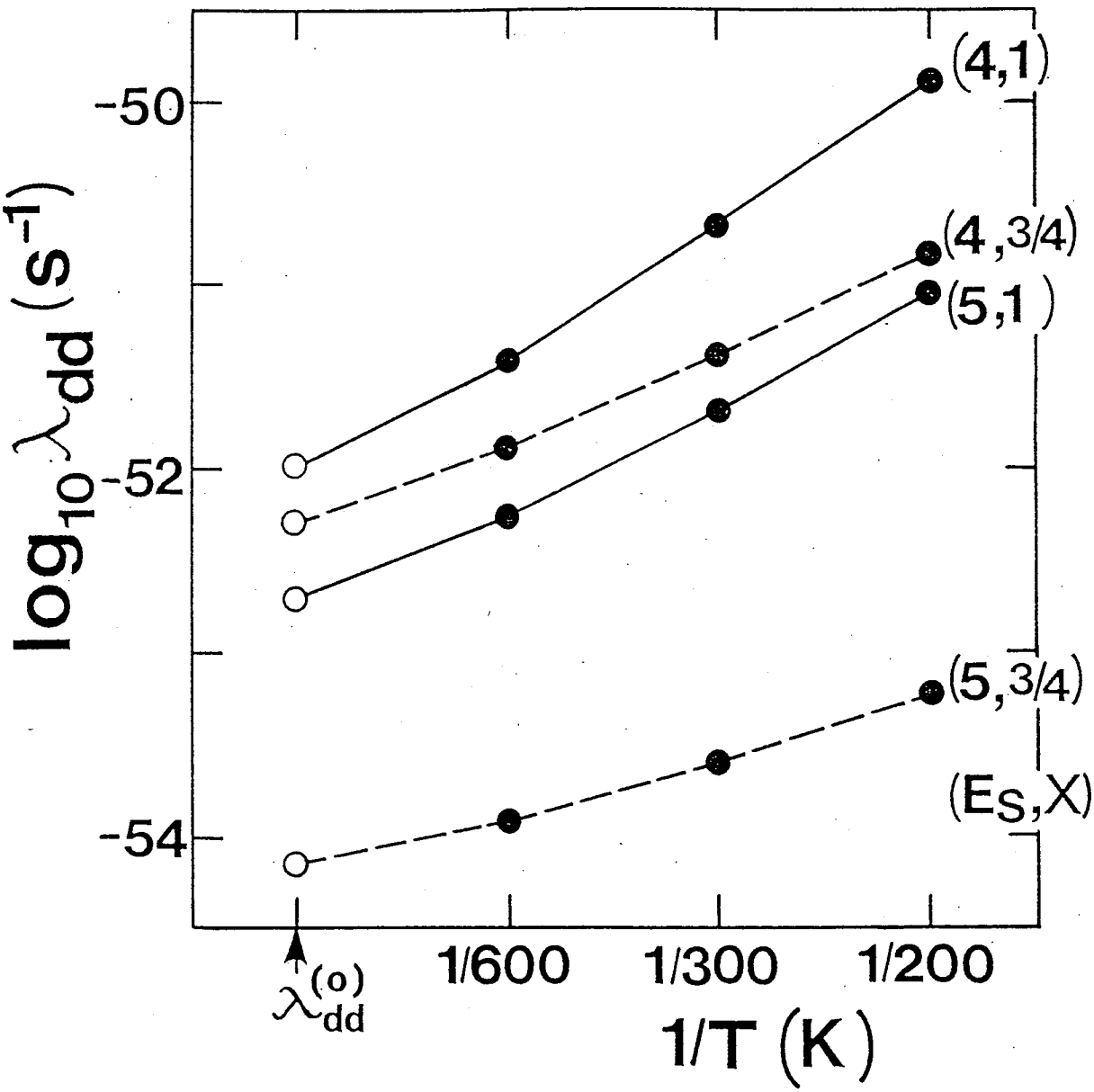

Fig. 3 S. Ichimaru et al.

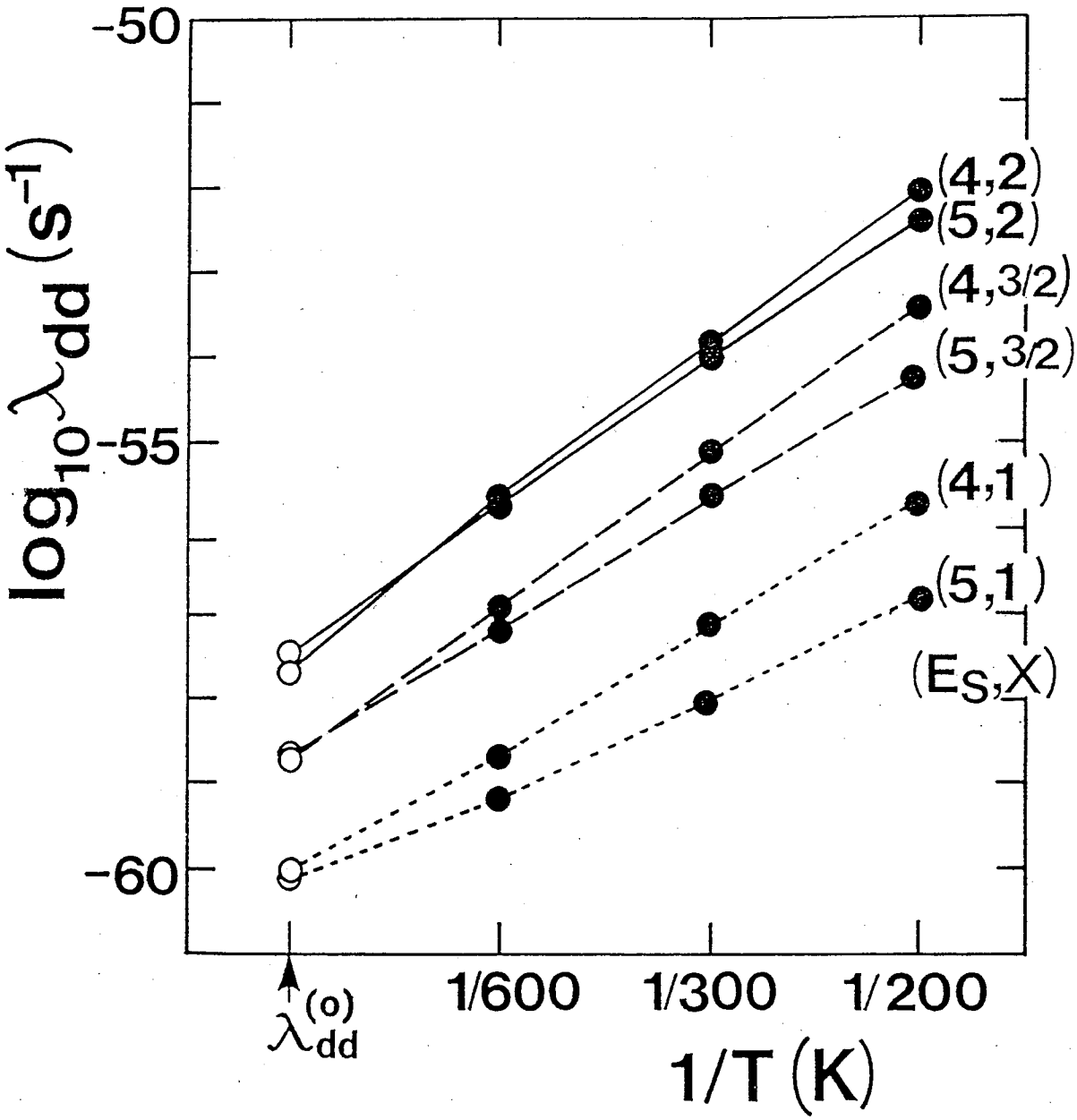

Fig. 4 S. Ichimaru et al.

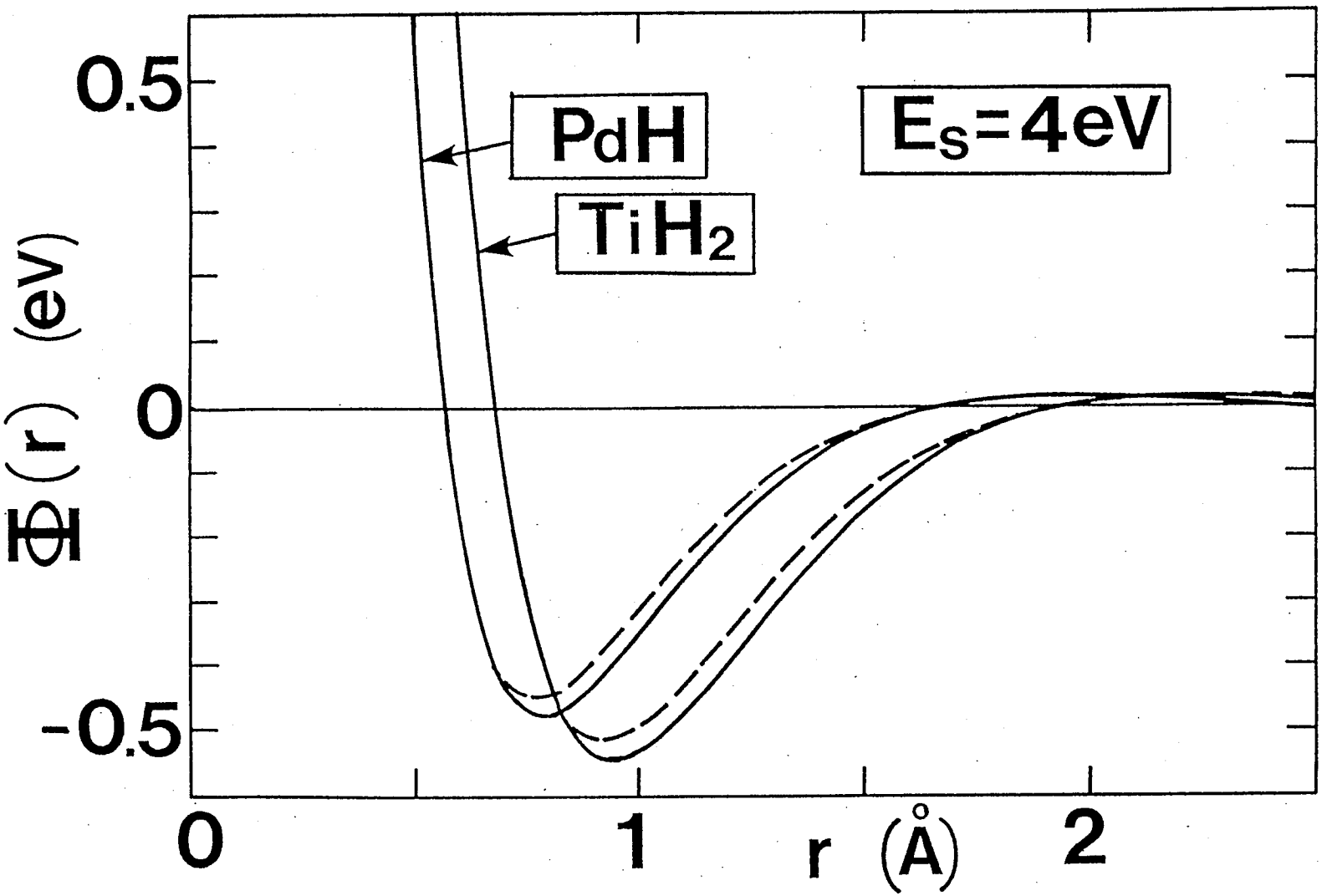

Fig. 5 S. Ichimaru et al.

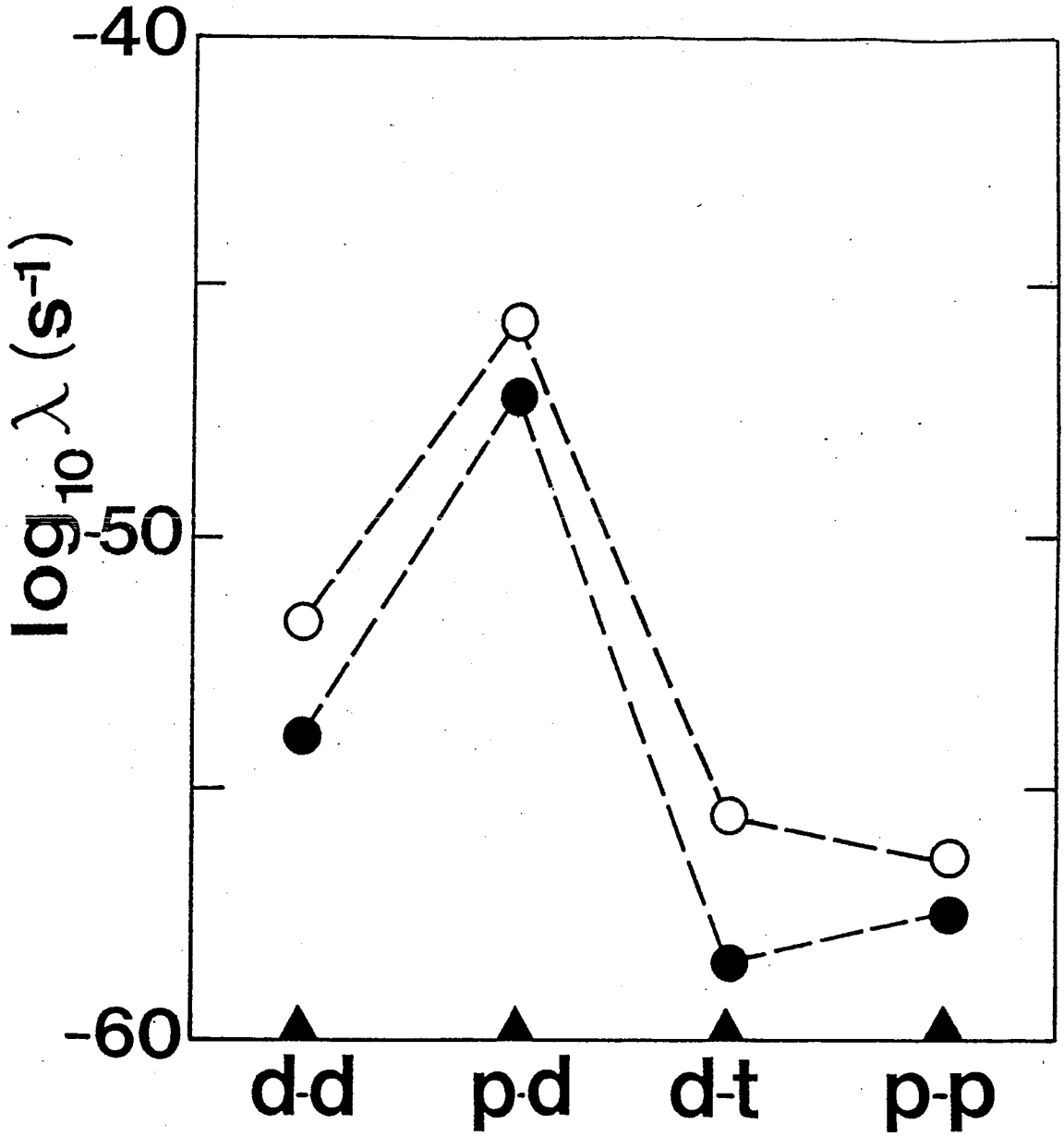

Fig. 6 S. Ichimaru et al.